

ROI Limited Unknowns Reduction based Contrast Source Inversion for Microwave Breast Imaging

Hiroki Sato, *Non-member* and Shouhei Kidera, *Member, IEEE*,

Abstract—This study introduces an accuracy-enhanced microwave imaging algorithm on the basis of contrast source inversion (CSI), aimed at a quantitative microwave breast cancer imaging scenario. The unknowns in the inverse scattering scheme form the most common difficulty in terms of providing an accurate dielectric profile with less measurement data. A region of interest (ROI) limitation and an updating scheme are developed in this study to reduce the number of unknowns. Numerical tests using several realistic breast phantom models demonstrate that our proposed method considerably enhances the reconstruction accuracy. The results show consistency even for typical situations where the amount of observed data is lower than the unknowns.

I. INTRODUCTION

Microwave imaging is a modality with significant advantages over the existing X-ray, magnetic resonance imaging (MRI), and ultrasound-based diagnostic techniques, providing safe, low-cost, harmless, and non-contact measurement. Global statistics reports indicate that breast cancer is one of the most morbid and mortal among all types of cancer cancers[1]. Microwave breast cancer screening has several advantages as mentioned above and is a promising method for more frequent and quantitative examinations, which enables the detection of the cancer in earlier stages than the other techniques. A large-scale investigation of *ex vivo* breast tissues, including tumors, revealed that there is a significant contrast of complex permittivity between cancerous and normal tissues (*e.g.*, adipose or fibro-glandular tissues) at microwave frequency band. These results have accelerated the development of microwave-based breast cancer detection systems in recent decades[2].

The microwave imaging approaches are typically developed in two categories. The first approach is the qualitative radar imaging scheme, which can be used to retrieve higher reflection coefficients from backgrounds by processing reflection responses from breast media, including cancer, with relatively low computational complexity [3]. However, it suffers from unnecessary responses because of the high dielectric contrast between the fibro-glandular tissue and the background adipose media. In this case, it becomes difficult to achieve an adequate screening performance, where the fibroglandular tissue is more dominant than the adipose one.

The second approach is based on inverse scattering analysis, also known as the tomographic approach, which offers quantitative dielectric profile. The tomographic approach must solve the ill-posed and nonlinear optimization problem, formulated

by the domain integration equation (DIE). The distorted Born iterative method (DBIM) is one of the most promising tomographic approaches [4]. The DBIM provides an accurate reconstruction result of dielectric profile even when dealing with densely heterogeneous media such as high contrast cancerous tissue. A number of studies have demonstrated the effectiveness of DBIM on breast tumor detection [5], [6]. However, this requires a high computational cost, especially for three-dimensional (3-D) problems [7], because it requires a recursive update of the Green's function and the total electric fields in the region of interest (ROI) using accurate forward solver such as the finite difference time domain (FDTD) method. Another technique, the contrast source inversion (CSI) scheme, has been developed [8] to avoid a computationally expensive forward solver. This is accomplished by sequentially updating the total field in the ROI by minimizing the residuals between the measured and the reconstructed scattered fields at both the observation and object areas, and it could avoid the use of the forward solver. CSI is currently one of the most promising reconstruction tools. Variations of the algorithm, including multiplicative regularization (MR)-CSI [8], [9], finite difference CSI (FD-CSI) [10], [11], or cross-correlated CSI (CC-CSI)[12] have been introduced to upgrade the reconstruction performance of the method. Many biomedical applications have been described in literature [13], [14], [15]. However, the applications are limited by the inaccuracy of complex permittivity reconstruction due to ill-posedness, particularly with regard to the amount of measured data being much less than the number of unknowns in a 3-D problem.

To overcome this issue, this paper focuses on a scheme for the reduction of the number of unknowns using the ROI limitation in the CSI framework. In this method, the unknown cells allocated to adipose tissues are regarded as the background medium and eliminated from the total unknowns using an initial estimate of the CSI. In this case, only the ROI with higher contrast, the fibro-glandular or cancerous areas, can be reconstructed by the sequential CSI scheme. A similar approach developed recently, namely, the level set functions approach [16], still requires accurate prior knowledge of the dielectric profile of each tissue, and there are only a few reports about dispersive breast media available in the literature. In this study, a numerical test using the two-dimensional (2-D) FDTD simulation with several types of realistic MRI-derived phantoms is investigated. The results show that our proposed method remarkably upgrades the reconstruction performance in all cases, including those in which the amount of measurement data is lower than the unknowns.

This research and development work were supported by the MIC/SCOPE #162103102.

H. Sato and S. Kidera are with Graduate School of Informatics and Engineering, The University of Electro-Communications, Tokyo, Japan. E-mail: kidera@uec.ac.jp

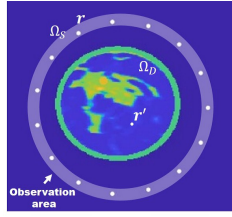


Fig. 1: Observation model.

II. METHOD

A. Observation model

Figure 1 illustrates the 2-D observation model. It assumes that a breast object is expressed as a mix of skin, adipose, fibro-glandular, and cancer tissues, with lossy, dispersive, and isotropic dielectric properties. A circular array composed of transmitters and receivers surrounds the breast object. The observation, where the array exists, is denoted by Ω_S , and the ROI is denoted by Ω_D . A multi-static observation model is used, which combines all data observed from the transmitter and the receiver. $E_{i,j,k}^T(\mathbf{r})$ and $E_{i,j,k}^{TB}(\mathbf{r})$ are denoted as total fields measured with and without object. In this case, the source current is excited by the i -th transmitter, and its scattered electric field is recorded at j -th receiver, whereas k denotes the frequency index.

B. Original CSI Method

This section briefly describes the electro-magnetic inverse scattering problem, formulated by the Helmholtz DIE. The recorded electric field in the observation area, denoted as Ω_S is expressed by the following equation:

$$\begin{aligned} E_{i,j,k}^S(\mathbf{r}) &\equiv E_{i,j,k}^T(\mathbf{r}) - E_{i,j,k}^{TB}(\mathbf{r}) \\ &= (k_k^B)^2 \int_{\Omega_D} G_{j,k}^B(\mathbf{r}') w_{i,k}(\mathbf{r}') d\mathbf{r}', (\mathbf{r} \in \Omega_S) \end{aligned} \quad (1)$$

where $E_{i,j,k}^S$ denotes the scattered electric field, and k_k^B and $G_{j,k}^B(\mathbf{r})$ are the wavenumber and the Green's function of the background media, respectively. Note that, $w_{i,k}(\mathbf{r}) \equiv E_{i,j,k}^T(\mathbf{r}) \chi_k(\mathbf{r})$ is introduced by using the contrast function denoted as $\chi_k(\mathbf{r}) \equiv \epsilon_k(\mathbf{r}) / \epsilon_k^B(\mathbf{r}) - 1$. Here, $\epsilon_k(\mathbf{r})$ and $\epsilon_k^B(\mathbf{r})$ denote the complex permittivities of an object and background media, respectively.

The problem for solving $\chi_k(\mathbf{r})$ is called the inverse scattering problem and is a well known ill-posed and nonlinear problem. To address the nonlinearity problem, various approaches have been developed, such as BIM, DBIM (equivalent to Gauss-Newton method), CS-EB, and CSI. The CSI scheme was selected for this study because of its advantages in terms of low computational complexity and reconstruction accuracy. The CSI considers another integration equation, which should be satisfied in the ROI rather than in the observation area:

$$\begin{aligned} w_{i,k}(\mathbf{r}) - \chi_k(\mathbf{r}) E_{i,j,k}^{TB}(\mathbf{r}) \\ = \chi_k(\mathbf{r}) (k_k^B)^2 \int_{\Omega_D} G_{j,k}^B(\mathbf{r}') w_{i,k}(\mathbf{r}') d\mathbf{r}', (\mathbf{r} \in \Omega_D) \end{aligned} \quad (2)$$

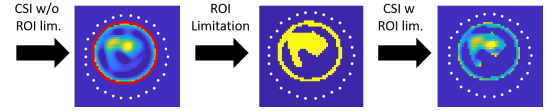


Fig. 2: Scheme of the ROI limited CSI algorithm.

where Ω_D denotes the ROI. Note that, Eq. (2) is known as "state equation", which is distinguished from Eq. (1) known as "data equation". The subscript j in Eq. (2) expresses the index number of cells allocated in the assumed ROI. Regarding Eqs. (1) and (2), the CSI solves the object functions χ and w alternatively by minimizing the following cost function at the specific frequency f_k :

$$\begin{aligned} F_k(\chi_k, w_k) &\equiv \frac{\sum_i \|E_{i,j,k}^S - (k_k^B)^2 \int_{\Omega_D} G_{j,k}^B w_{i,k} d\mathbf{r}'\|_S^2}{\sum_i \|E_{i,j,k}^S\|_S^2} \\ &+ \frac{\sum_i \|\chi_k E_{i,j,k}^{TB} - w_{i,k} + \chi_k (k_k^B)^2 \int_{\Omega_D} G_{j,k}^B w_{i,k} d\mathbf{r}'\|_D^2}{\sum_i \|\chi_k E_{i,j,k}^{TB}\|_D^2}, \end{aligned} \quad (3)$$

where $\|\cdot\|_S^2$ and $\|\cdot\|_D^2$ denote the l_2 norms of the regions Ω_S and Ω_D , respectively. This method has a notable advantage over methods such as DBIM because it avoids an iterative updates of the total fields in the ROI by the forward solver (such as the FDTD method), and remarkably reduces the computational cost and memory needed to obtain a reconstruction profile. Instead of the forward solver, the total field in the ROI is sequentially updated by minimizing the cost function in Eq. 3.

C. Proposed Method : ROI Limited CSI Method

The original CSI has been applied to various types of observation models, and its effectiveness has been demonstrated. Nevertheless, it has a substantial tendency toward ill-posedness, in particular for 3-D models, where the amount of observation data is much lower than the unknowns. To overcome this issue, this study introduces the limited ROI and its updating scheme to the CSI framework. The proposed technique focuses on the well-established fact that the adipose tissue is the most dominant in the breast medium, ranging from 50 % to 80 % [17]. Initial estimates are used to determine the adipose tissue area, which is then included in the background medium, significantly reducing the number of unknowns. In this way, the proposed process can be used to enhance the reconstruction accuracy for the area with a relatively higher complex permittivity than the background, i.e., the fibro-glandular or cancerous tissues. Figure 2 illustrates the schematic diagram of the ROI limitation and updating process. The detailed procedures of the proposed method are summarized in the steps below.

- 1) Assuming a whole breast area as the ROI, the CSI is applied to the observed data until a specific number of iterations. In this case, its initial reconstruction profile is denoted as $\tilde{\epsilon}(\mathbf{r})$.
- 2) The ROI is updated as $\tilde{\Omega}_D$, which satisfies the following condition:

$$\tilde{\Omega}_D = \{\mathbf{r} \mid \text{Re}[\tilde{\epsilon}(\mathbf{r})] \geq \epsilon_{\text{th}}\} \quad (4)$$

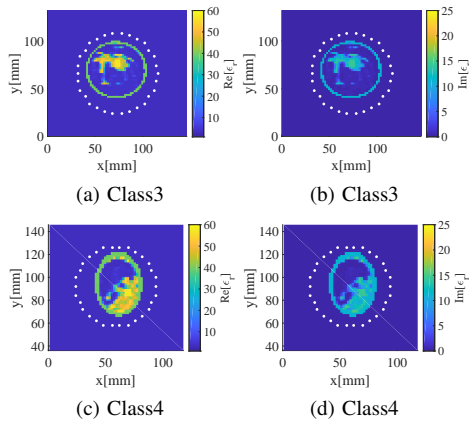


Fig. 3: Original profile of complex permittivity. (a) and (c): Real part. (b) and (d): Imaginary part.

where ε_{th} denotes the threshold of complex permittivity, which should be higher than that of background medium, namely, an adipose tissue.

- 3) CSI with updating ROI. The CSI inversion is now performed by minimizing the following updated cost function:

$$F'_k(\chi_k, w_k) \equiv \frac{\sum_i \|E_{i,j,k}^S - (k_k^B)^2 \int_{\tilde{\Omega}_D} G_{j,k}^B w_{i,k} dr\|_S^2}{\sum_i \|E_{i,j,k}^S\|_S^2} + \frac{\sum_i \|\chi_k E_{i,k}^{TB} - w_{i,k} + \chi_k (k_k^B)^2 \int_{\tilde{\Omega}_D} G_k^B w_{i,k} dr\|_D^2}{\sum_i \|\chi_k E_{i,k}^{TB}\|_D^2}. \quad (5)$$

Note that, $\|\cdot\|_D^2$ is replaced using the $\tilde{\Omega}_D$.

- 4) Go back to Step 2) and repeat Step 2) to Step 4, until the number of iteration would reach the upper limitation.

As described in the above procedure, this method does not require any prior knowledge of breast media. If the initial estimate is accurate, the ROI can be correctly limited, resulting in the improvement of the reconstruction accuracy.

III. RESULTS AND DISCUSSIONS

The 2-D FDTD numerical tests were investigated where a realistic numerical phantom quantized by the MRI image was introduced [17]. To determine the relevance of the method, two different types of breast models were examined, namely, the class 3 (heterogeneously dense) and class 4 (very dense) phantoms. Figure 3 illustrates the original profiles for each class phantom, each containing small cancerous tissues of 6 mm square with $\varepsilon_r = 56.7 - j14.1@2.0$ GHz [18]. A raised-cosine pulse with a center frequency of 2.0 GHz and a bandwidth of 2.1 GHz was excited as a current source. The 30 source and observation points are set at the surrounding area of the breast. The dispersive FDTD code developed by the University of Wisconsin–Madison, which assumes the single-pole Debye model, was used to simulate the scattered field. In this case, the cell size of the FDTD and the unknown pixel within CSI are both 2 mm. Here, the noiseless case was assumed. The dielectric profile of background was set to $\varepsilon_k^B = 3.3 - j0@2.0$ GHz, which approximately corresponds to the adipose tissue.

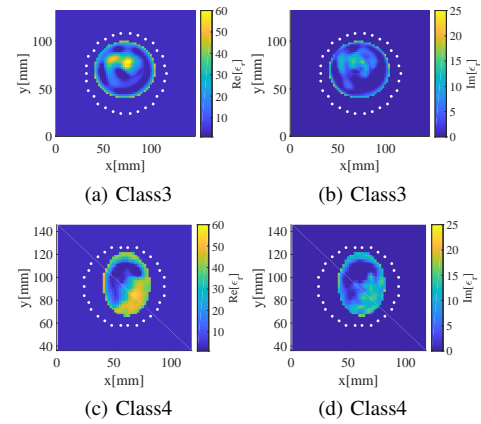


Fig. 4: Reconstruction results by the original CSI (without ROI limitation). (a) and (c): Real part. (b) and (d): Imaginary part.

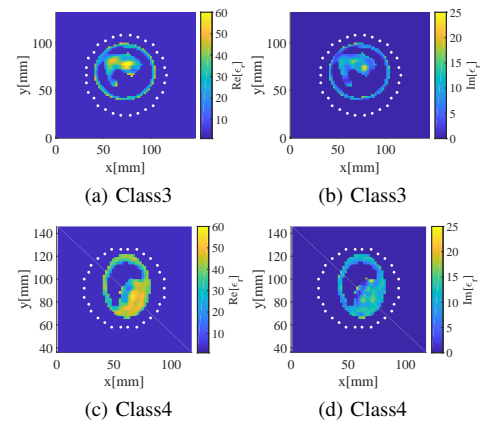


Fig. 5: Reconstruction results by the proposed CSI (w ROI limitation). (a) and (c): Real part. (b) and (d): Imaginary part.

Figure 4 illustrates the initial reconstruction results when using the CSI without the ROI limitation, where the number of iteration step is set to 30000. In this case, the whole breast area is processed as the ROI and shows that the initial guess provides a relatively good reconstruction of the outlines of the low and high permittivity areas. However, its reconstruction accuracy is insufficient to recognize the cancer cells. In contrast, the proposed method using the ROI limitation and updated CSI scheme provides a more accurate dielectric profile, especially for the high contrast areas (including the cancerous tissue), as shown in Figure 5. Note that the threshold $\varepsilon_{th} = 13$ in Eq. (4) is set. The number of unknowns in class 3 are 729 and 356 in w/o and w ROI limitation, and those in class 4 are 458 and 311 in w/o and w ROI limitation. Figure 6 shows the one-dimensional (1D) cross section of the reconstruction results for Class 3 for each plane. The results show that compared with the conventional CSI, our proposed method, CSI with ROI limitation, provides a more accurate profile, especially for higher contrast tissues. Finally, Table I summarizes the cumulative probabilities at the specific error criteria and demonstrates that the proposed method considerably enhances the reconstruction accuracy in any class by reducing the number of unknowns.

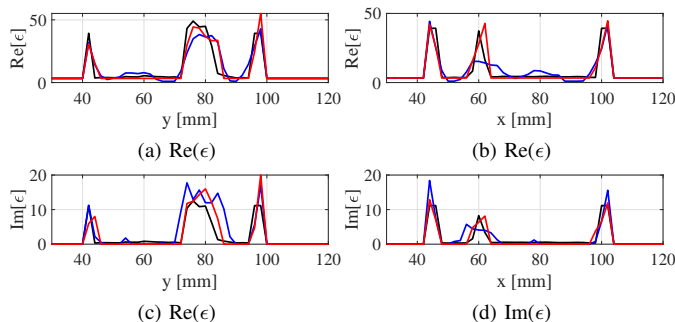


Fig. 6: Cross-sectional reconstruction results at Class 3 case in noise-free case. (a) : $x = 68$ mm. (b) : $y = 58$ mm. Black line denotes the original profile. Blue and red solid lines denote the reconstruction profiles by the original and the proposed CSIs, respectively.

TABLE I: Cumulative probabilities, satisfying the errors are within ± 3 and ± 1 from the original real and imaginary parts, respectively.

		Class3	Class4
Re[ϵ_r]	CSI w/o ROI lim.	33.9%	38.4%
	CSI w ROI lim.	61.1%	55.7%
Im[ϵ_r]	CSI w/o ROI lim.	46.7%	38.0%
	CSI w ROI lim.	60.8%	75.3%

TABLE II: Cumulative probabilities at each SNR level in Class 3 phantom, where same criteria in Table. I is used.

		SN=30 dB	SN=20 dB	SN=10 dB
Re[ϵ_r]	CSI w/o ROI lim.	33.3 %	33.1 %	30.2 %
	CSI w ROI lim.	54.0 %	54.0 %	53.8 %
Im[ϵ_r]	CSI w/o ROI lim.	47.6 %	46.0 %	46.0 %
	CSI w ROI lim.	53.5 %	53.5 %	55.2 %

Further, we demonstrated the impact of noise on the proposed method by examining Class 3 as the representative. Here, we added white Gaussian noise to both recorded scattered fields, as reported by an earlier study [19]. The power of the signal was defined as the maximum power of the received signals, and these signals were mostly dominated by surface reflection from the skin. Figure 7 shows the reconstruction results for each method at an SNR of 10 dB, and Table II lists the cumulative probability values for comparison (the error criteria are the same as that in Table I. These results show that our proposed method has a significant advantage over the original CSI even under noisy conditions because redundant data suppress fluctuations due to noise via the averaging effect when we can reduce the number of unknowns.

Finally, we examined the dependency of the reconstruction result on the threshold ϵ_{th} . Figure 8 shows the reconstruction profiles for different ϵ_{th} in a Class 3 case in a noise-free scenario. The figure shows that the results are not highly sensitive to the threshold. In general, if we increase ϵ_{th} , higher contrast issues are included in the background adipose tissues, thereby worsening the performance. On the other hand, if ϵ_{th} is set as a smaller value, there is no clear benefit because of the insufficient reduction of the number of unknowns. Therefore, it is necessary to maintain a balance and determine the optimal ϵ_{th} considering the dielectric constant between the background adipose and high-contrast fibroglandular tissues.

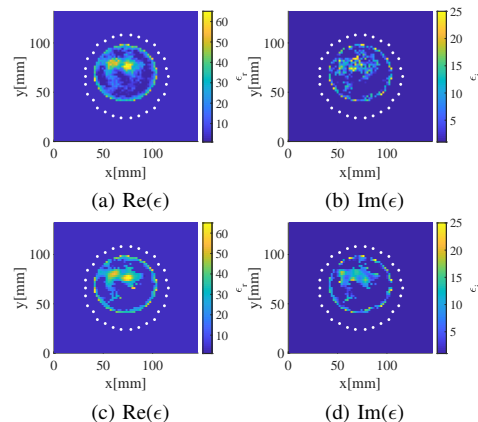


Fig. 7: Reconstruction results in Class 3 of SNR = 10 dB. (a) and (b): Original CSI, (c) and (d): Proposed CSI.

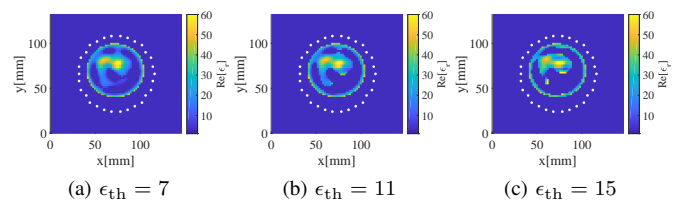


Fig. 8: Reconstruction results of real part of complex permittivity by the proposed CSI, where the ϵ_{th} is changed, at noise-free case.

IV. CONCLUSION

This study introduces a CSI scheme with the accuracy enhanced by the reduction of the number of unknowns based on ROI limitation. This study focuses on the fact that the adipose tissue area is the most dominant in a typical breast medium, which was then included in the background medium to eliminate the unknowns. The scheme was accomplished by assessing the initial estimate of CSI without the ROI limitation and then reforming the cost function in the CSI. The FDTD-based numerical tests, assuming various realistic breast phantoms, demonstrated that our scheme successfully enhances the reconstruction accuracy even when a low amount of observation data is available. If the number of iterations in the initial estimate is insufficient, the reconstruction performance worsens because of the inappropriate limitation of the ROI. Hence, we need to set the appropriate convergence criteria in Step (1) of the proposed method. Furthermore, the ill-posedness of this inversion problem becomes extremely critical in the 3-D model or realistic case owing to a significant increase in the number of unknowns. Therefore, it is very important task to implement the 3-D numerical or experimental validations in the near future.

REFERENCES

- [1] F. Bray, J. Ferlay, I. Soerjomataram, R. Siegel, L. Torre, and A. Jemal, "Global cancer statistics 2018: GLOBOCAN estimates of incidence and mortality worldwide for 36 cancers in 185 countries," *Cancer Jnl. for Clinicians*, vol. 68, no. 6, December 2018, pp. 394–424, doi: 10.3322/caac.21492.

- [2] M. Lazebnik, D. Popovic, L. McCartney, *et al.*, "A large-scale study of the ultrawideband microwave dielectric properties of normal, benign and malignant breast tissues obtained from cancer surgeries," *IOP Publishing Phys. Med. Biol.*, vol. 52, 2007, pp. 2637–2656, doi: 10.1088/0031-9155/52/20/002.
- [3] E. J. Bond, Xu Li, and S. C. Hagness, "Microwave imaging via space-time beamforming for early detection of breast cancer," *IEEE Trans. Antennas Propagat.*, vol. 51, 8, August 2003, pp. 1690–1705, doi: 10.1109/TAP.2003.815446.
- [4] W. C. Chew and Y. M. Wang, "Reconstruction of two-dimensional permittivity distribution using the distorted Born iterative method," *IEEE Trans. Med. Imag.*, vol. 9, pp. 218–225, June 1990.
- [5] J. D. Shea, P. Kosmas, S. C. Hagness and B. D. Van Veen., "Three-dimensional microwave imaging of realistic numerical breast phantoms via a multiple-frequency inverse scattering technique," *Am. Assoc. Phys. Med.*, vol. 37, no. 8, August 2010, pp. 4210–4226, doi: 10.1118/1.3443569.
- [6] K. Noritake and S. Kidera, "Boundary Extraction Enhanced Distorted Born Iterative Method for Microwave Mammography," *IEEE Antennas and Wireless Propagation Letters*, vol. 18, 4, April 2019, pp. 776–780, doi: 10.1109/LAWP.2019.2902351.
- [7] K. Noritake and S. Kidera, "Three-dimensional Distorted Born Iterative Method Enhanced by Breast Boundary Extraction for Microwave Mammography," *2019 41st Annual International Conference of the IEEE Engineering in Medicine and Biology Society (EMBC)*, 2019, pp. 4819–4823.
- [8] P. M. van den Berg and A. Abubakar, "Contrast Source Inversion Method: State of Art," *Progress In Electromagnetics Research, PIER* 34, 2001, pp. 189–218, doi: 10.2528/PIER01061103.
- [9] A. Zakaria and J. LoVetri, "Application of Multiplicative Regularization to the Finite-Element Contrast Source Inversion Method," *IEEE Trans. Antennas & Propagat.*, vol. 59, no. 9, pp. 3495–3498, Sept. 2011.
- [10] A. Abubakar, W. Hu, P. M. van den Berg, and T. M. Habashy, "A finite-difference contrast source inversion method," *Inverse Problems*, vol. 24, pp. 1–17, 2008.
- [11] C. Gilmore, A. Abubakar, W. Hu, T. M. Habashy and P. M. van den Berg, "Microwave Biomedical Data Inversion Using the Finite-Difference Contrast Source Inversion Method," *IEEE Trans. Antennas & Propagat.*, vol. 57, no. 5, pp. 1528–1538, May 2009.
- [12] S. Sun, B. J. Kooij, T. Jin and A. G. Yarovoy, "Cross-Correlated Contrast Source Inversion," *IEEE Trans. Antennas & Propagat.*, vol. 65, no. 5, pp. 2592–2603, May 2017.
- [13] A. Abubakar, P.M. van den Berg, and J.J. Mallorqui, "Imaging of biomedical data using a multiplicative regularized contrast source inversion method", *IEEE Trans. Microwave Theory & Techniques*, vol. 50, no. 7, pp. 1761 - 1771, Jul., 2002.
- [14] N. Ozmen-Eryilmaz and K. W. Van Dongen "A contrast source inversion method for breast cancer detection" *Proc. Mtgs. Acoust.* 19, 075003 2013.
- [15] H. Sato and S. Kidera, "Multi-frequency Integration Algorithm of Contrast Source Inversion Method for Microwave Breast Tumor Detection" 41st IEEE International Engineering in Medicine and Biology Conference 2019 (IEEE EMBC 2019), Berlin, Germany, July, 2019.
- [16] Oliver Dorn and Dominique Lesselier, "Level set methods for inverse scattering," *Inverse Problems*, vol. 22, no. 4, June 2006, pp. R67–R131, doi: 10.1088/0266-5611/22/4/R01.
- [17] UWCEM, "Numerical breast phantom repository", URL: <https://uwcem.ece.wisc.edu/phantomRepository.html>
- [18] F. Gao, B. D. Van Veen, and S. C. Hagness, "Sensitivity of the Distorted Born Iterative Method to the Initial Guess in Microwave Breast Imaging," *IEEE Trans. Antennas Propagat.*, vol. 63, no. 8, August 2015, pp. 145–154, doi: 10.1109/TAP.2015.2436406.
- [19] J. D. Shea, P. Kosmas, B. D. Van Veen, and S. C. Hagness, "Contrast enhanced microwave imaging of breast tumors: a computational study using 3-D realistic numerical phantoms", *Inverse Probl.*, 2010;26(7):74009.